

Development of the SPACE Lab Thrust Stand for Millinewton Thrust Measurement

IEPC-2019-715

*Presented at the 36th International Electric Propulsion Conference
University of Vienna, Austria
September 15-20, 2019*

Peter Thoreau* and Justin Little[†]
University of Washington, Seattle, WA, 98105, USA

The direct measurement of thrust to high precision is a key factor in the characterization of electric propulsion system performance. To provide this capability, a thrust stand has been built for the SPACE Lab (Space Propulsion and Advanced Concepts Engineering Lab) at the University of Washington. The stand utilizes an inverted pendulum design with the thruster nested within the pendulum arms. The design allows for greater sensitivity within the limitations of the testing facilities, resulting in a wide range of steady thrust measurement from $100\mu\text{N}$ - 100 mN . The sensitivity is achieved across this range through modularity of the flexure assemblies. This gives the SPACE lab the capability to test the full range of operational and planned steady thrusters. The eddy current damper is adjustable against a predetermined power dissipation curve to allow both tunable damping and setup for new thrusters with minimal turnaround time. The system is semi-automated; before testing it generates a calibration curve for the stand and adjusts the leveling to the pendulum zero point. Initial tests of the system have been run using a cold gas thruster showing a linear and repeatable response across the full desired thrust range.

Nomenclature

\dot{m}	= Mass Flow Rate	g_0	= Gravity
ρ	= Density	I_f	= Second Moment of Area of the Flexure
θ_p	= Pendulum Deflection Angle	L_f	= Length of a Flexure
A	= Nozzle Area	L_p	= Length of the Pendulum Arm
B_P	= Peak Magnetic Field	m_t	= Total mass of the Pendulum and Thruster
d	= Distance Between Plates	P_a	= Atmospheric Pressure
E_f	= Young's Modulus of the Flexure	P_e	= Exhaust Pressure
f	= Frequency of Pendulum Oscillation	R	= Resistivity
F_T	= Thrust	v_{ex}	= Exhaust Velocity
F_{ss}	= Steady State Force		

*Graduate Student, Aeronautics & Astronautics, pthoreau@uw.edu.

[†]Assistant Professor, Aeronautics & Astronautics , littlej7@uw.edu

I. Introduction

The characterization of electric propulsion systems presents a significant challenge during their development. Of particular interest is the direct measurement of thrust, a difficult to obtain measurement due to the limitations of the test environment and thrust/weight ratios as low as 1/1000 [1]. While chemical rockets are able to utilize load cells for direct measurement, electric propulsion systems typically rely on the motion of a pendulum to separate the effects of gravity and thrust [2]. Three main conceptual designs of thrust stands are typically used for electric propulsion systems: hanging, inverted, and torsional pendulums. The designs, see figure 1, can also have additional factors such as double and counter-weighted pendulums [1, 3].

However, the sensitivity of the thrust stand is now directly proportional to the deflection, and therefore the length of the pendulum arm. As a result, their size is now a primary restriction to their sensitivity. If we also consider facility effects, which are minimized by centering the plume within the chamber, the available length for a thrust stand pendulum is further reduced [4].

Thrust stands typically target a set range of thrust levels for the systems they will measure. The range is derived from the restoring force on the stand and the maximum deflection. Due to the low power to weight ratios, the lowest thrust levels ($nN - \mu N$) use torsional pendulums which provide the highest sensitivity levels and restrict motion to a plane perpendicular to gravity. They can be suspended by torsion flexures, thin filament, or be even magnetically levitated to minimize external forces [5]. Inverted and hanging pendulums are more typically used for measurements above 1 mN [2]. Greater sensitivity can be derived from an inverted design as gravity acts to amplify the deflection [6]. Hanging pendulums are more commonly used for simpler designs, although they have been used with the addition of mechanical amplification across a broad range of thrust levels [7].

The use of electric propulsion systems, particularly in commercial space, has evolved significantly since the first commercial EP satellite was launched in 1993. While early EP systems were primarily used for GEO satellite station-keeping and deep space exploration; decreasing satellite research and development, production, launch, and operating costs have driven a move towards larger numbers of smaller satellites [8]. Electric propulsion in LEO is a mission enabler, allowing for orbit changing, drag compensation [9] and constellation flying [10]. The result of these innovations is a broad range of EP systems being developed, many of which don't require the facility size used for testing their larger counterparts. Therefore, this testing can be completed in smaller facilities with the added benefit of faster turnaround due to their smaller volumes. These systems require thrust characterization and thrust measurement, but may be limited by the available space for a pendulum arm to give sufficient sensitivity.

The SPACE Lab (Space Propulsion and Advanced Concepts Engineering Lab) at the University of Washington has several thrusters under development and therefore requires a thrust stand capable of measuring low thrust 10 W systems to high thrust 1 kW systems. This presents a significant challenge to capture such a wide range of thrust measurements which span the two regions dominated by vertical and torsional configurations. This paper describes the analysis and demonstration of a new compact, modular thrust stand, designed to make more efficient use of smaller test facilities without sacrificing sensitivity.

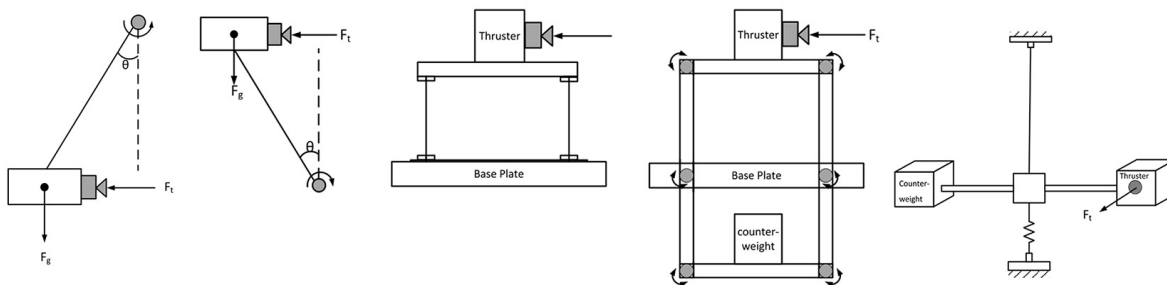


Figure 1: The standard configurations used for thrust stands. From left to right: Hanging Pendulum, Inverted Pendulum, Double Inverted Pendulum, Counterbalanced Inverted Pendulum, and Torsional Thrust Stands [1]

II. Thrust Stand Design

To drive the thrust stand design process towards achieving high sensitivity and thrust range in a compact design, the key performance metrics of the must be understood. Specifically, we designed the thrust stand to maximize the metrics set out by Polk et al., 2017 [2]:

- Sensitivity and Resolution: The ability of the thrust stand to measure thrust as a combination between the deflection for a given thrust and the capacity to measure that deflection. High sensitivity to low levels of thrust depends strongly on the vibration noise of the environment.
- Repeatability and Long Term Stability: The time evolution of the thrust measurement during long duration tests. Errors are due to the effects of heating, parasitic forces, friction and drift. Repeating the calibration before and after tests is used to check for this.
- Accuracy and Predictability of the Response: The relation between the measured thrust and the true thrust. Accuracy and predictability are improved through the minimization of systematic errors.

The requirements and restrictions to the design stem from both the performance targets, and the thrusters and facilities used. The base requirements for the stand are set to future proof the design and allow it to be used for thrusters between 10 W and 1 kW. A broad range of efficiencies were taken into account with a range of thrust/power ratios between 10 - 100 mN/kW [11]. This sets the requirement for steady state measurements from $100 \mu\text{N}$ to 100mN . The thrust stand was designed to accommodate a range of thrusters up to 42 cm in diameter, the size of a 1 kW gridded ion thruster, and have a range of propellants, data, and power connections, including RF. The pendulum was designed minimize the deflection of the thruster, both angular and normal to the thrust vector, so thrust measurements and beam diagnostics can be conducted simultaneously.

The vacuum chamber that will house the thrust stand is the Space Test Facility (STF). The STF uses a 1.45 m spherical chamber with flattened ends which has recently been extended by 1.7 m. The extension to the chamber adds additional volume and pumping capacity from a turbopump and up to 5 cryopumps. In order to maximize the range of thrusters that can be tested, and to efficiently use the space, the thrust stand was designed to position the thruster close to the door of the spherical chamber, see figure 2. This centers the plume within the chamber and gives maximum room for beam characterization before the beam dump. The separation minimizes facility effects due to pressure and return of sputtered material from the test chamber which decays exponentially with thruster separation to the wall [4]. This will be particularly important for the testing of larger thrusters closer to the upper limit of the stand and STF.

While literature surveys showed that thrust stands exist with the desired range of measurement, a distinct lack of designs that were small enough were available. Figure 3 shows a selection of thrust stands near the relevant region of size and range. Here, the characteristic size is defined as the smallest radius cylindrical chamber the device can be tested in while maintaining a centered plume.

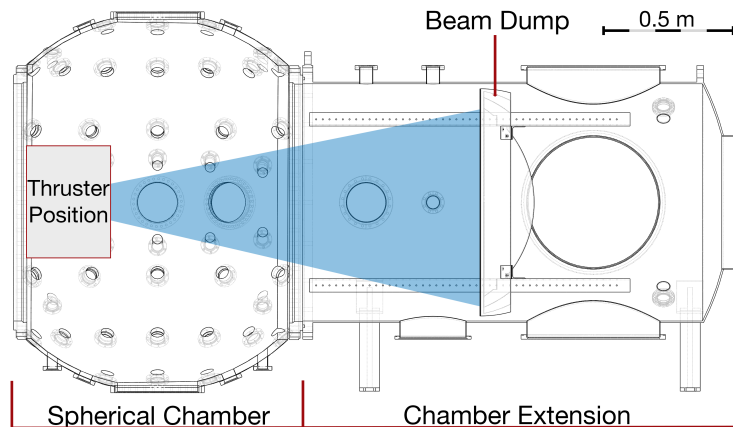


Figure 2: The SPACE Lab STF showing the optimal thruster position, with the plume, and beam dump.

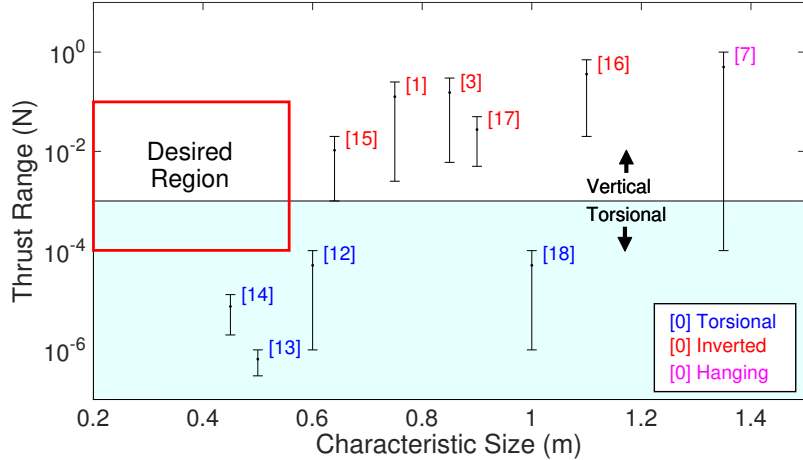


Figure 3: A review of current thrust stands comparing their thrust measurement range to their size. Data is from published test results, actual ranges are likely larger. [1, 3, 7, 12–18]

A delineation of vertical vs torsional system is shown clearly dividing the stands surveyed between torsional and inverted pendulum. Only one hanging pendulum is shown, [7], which uses mechanical amplification and a long pendulum arm to increase its base sensitivity. The divide shown between the ranges is not absolute, as torsional systems have been built with ranges in the N [19], however examples of this are rare. The desired region has no examples from literature and crosses between vertical and torsional system dominance, giving no clear indication of which design should be selected.

A. Design Overview

To meet the performance requirements while maintaining a small characteristic size required a novel approach. The performance metrics defined by Polk et al., 2017, along with the requirements and restrictions were used as the base of a trade off study comparing the fundamental types of thrust stand. The trade off also considered: the complexity of the design, complexity of the assembly and operation, sizing for the chamber, and cost. While each of these designs were constrained by several factors, a double inverted pendulum best suited the application.

In a traditional inverted pendulum, the thruster sits on top of the stand. However to increase the sensitivity and range, without significantly increasing size, the thruster is moved to nest within the pendulum arms. This reduced the characteristic size to under 0.4 m while keeping the sensitivity of a 0.8 m system. However, care must be taken with the thermal shroud and watercooling system to ensure this approach does not cause significant thermal error due to the increased surface area the thruster can radiate to.

Although the fundamental principle of the inverted pendulum does not restrict its usage at the $\approx 100 \mu\text{N}$ thrust level, previous examples of its use at this range are limited. Therefore, to predict the response and guide the design of the flexures and pendulum, the system was modeled both analytically in Matlab, and in Solidworks using FEA. The analytical model of the response due to an applied thrust is made up of the second moment of area combined with the idealized beam bending of the flexures and takes advantage of the symmetry of the system in all 3 axis. The deflection in steady state is calculated from the steady state force F_{ss} due to the thrust, F_T , and gravity, g_0 , acting on the thruster mass m_t :

$$F_{ss} = F_T + \theta_p m_t g_0 \quad (1)$$

Where the deflection angle θ_p is calculated iteratively with the pendulum and flexure lengths, L_p and L_f , and the Young's modulus and second moment of area of the flexures, E_f and I_f :

$$\theta_p = F_{ss} \frac{L_p L_f}{16 E_f I_f} \quad (2)$$

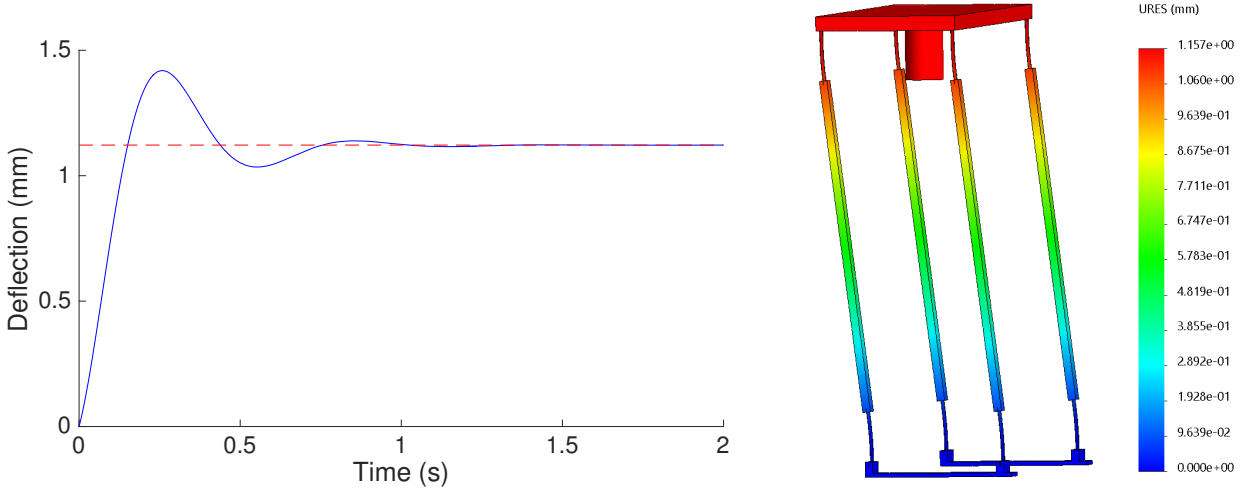


Figure 4: a) The analytical model predicting the response to 20 mN thrust from a 1 kg thruster with 0.5 mm flexures and a damping coefficient of 0.4. b) The FEA model with the same parameters showing the estimated deflection of 1.16 mm.

The movement is then modeled as a damped harmonic oscillator where the damping factor comes from the approximated power dissipation of the eddy current damper described in section E. The FEA model, see figure 4b was used primarily as a confirmation that the analytical model was approximately correct and could be used for further design.

B. Pendulum and Flexures

The pendulum and flexures are the primary components of the thrust stand. There are 4 pendulum arms with a total of 8 flexures, see figure 5a. The configuration ensures that the top of the pendulum remains level and with minimal vertical deflection, while remaining stable and low profile, allowing it to sit close to the end of the chamber. The predictability of the response over a large range of thrust measurements require a modular system of flexures of varying thickness and therefore stiffnesses. The flexures are made of spring steel, Laser cut on a 1kW Coherent Meta 10C Laser from sheet stock. Using the analytical model and a standardized rectangular shape, flexures ranging from 0.15 to 0.65 mm thick were cut to give a thrust range of 10 μ N to 150 mN. The maximum deflection in the flexures is well within the limits for elastic deformation for the material ensuring repeatable measurements and minimal zero point drift.

A rigid frame is required to transfer the thrust to the flexures and mount the damping and measurement systems. The truss design used for the top of the pendulum and the T bars used for the arms give sufficient stiffness while maintaining low mass. The assumption of rigidity in the system holds for forces into the 10's of Newtons, well beyond the designed upper limit. If the system was required to extend beyond these regions, a replacement to the standard pendulum frame would be needed. An additional check within the code outputs a buckling safety factor and maximum loading recommendation when calculating each response curve.

C. Structure

The full thrust stand system is composed of 3 primary structures, see figure 5b. The first of the base frames sits within the spherical chamber on vibration damping rubber mounts. It is removable from the chamber allowing for cleaning or other experiments which may require the full volume. The frame mounts the main translation stage in the chamber and supports the linear stepper motors used to level the second frame. The second frame is mounted on the lower frame by three points. One ball pivot and the two linear stepper motors, all of which incorporate an additional layer of vibration isolation to reduce the noise floor the stand experiences. The stepper motors level the stand in 2 axes using the zero point of the pendulum as the primary sensor. The watercooling shroud and rails are mounted to this frame, keeping them level

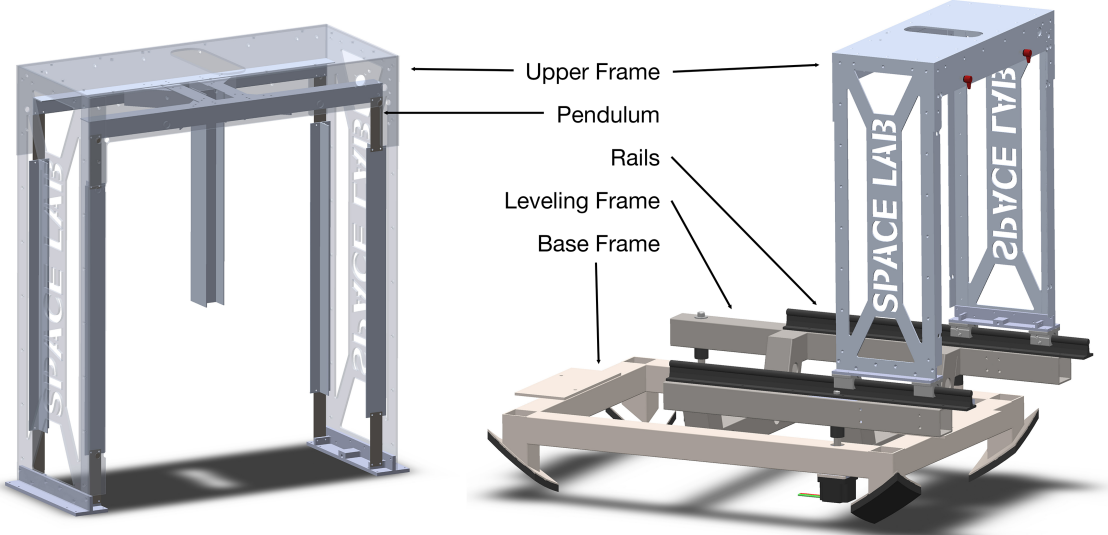


Figure 5: a) The upper frame (translucent) showing the layout of the pendulum and 8 flexures. b) The three frames for the thrust stand including the rails and locking mechanism.

and located relative to the thrust stand. The upper frame surrounding the pendulum is used as an end stop, at the limits of the linear regime, and to mount the measurement and calibration systems. It connects to the pendulum through the mounting block at the base and through a locking system at the top of the structure. The mounting block also houses the linear bearings used to run the upper frame along the rails. The locking system holds the pendulum securely in place allowing for it to be moved without causing damage to the flexures or thruster. This isolation allows flexures to be swapped quickly and easily while maintaining alignment and without introducing anisotropy due to torsion or misalignment of the pendulum arms.

Propellant, power and data connections are fed to the thruster using a waterfall configuration. The non-linear effects on the equivalent spring constant caused by these connections are minimized in two ways. Firstly, the waterfall head is set well above the thruster minimizing the change in angle, and ensuring that expansion and contraction forces are normal to the thrust vector. And secondly, connections and feeds are as flexible as possible. Similar designs have seen errors in the range of $\pm 0.6\%$ of full scale calibration [20].

D. Measurement system

The thrust measurement is derived from the deflection of the stand and the assumption of linearity allowing for interpolation of the calibration curve. The sensitivity and resolution of the system is the combination of the flexure stiffness and the resolution of the laser. The pendulum position is measured by a Keyence IL-100 Laser in 655 nm. The output, read by an IL-1000 amplifier unit, can measure the full range of deflection of ± 5 mm and remain linear to within 0.15% with a repeatability of $4 \mu\text{m}$ at a sampling rate of 1000 s^{-1} . The laser is mounted to the inside of the upper frame where it is shielded from any plume or temperature effects by the watercooling shroud. A diffuse white target for the laser is mounted to the top of the pendulum which is also shrouded. The thrust sensitivity is dependant on the flexures setup, while the deflection sensitivity is set at 350 mV/mm.

E. Damping system

For continuous thrust measurements, the deflection needs to reach a steady state value. The low resistance of the pendulum will allow it to oscillate for long periods of time. During early tests the pendulum oscillated continuously for 15 minutes, even with the damping of atmosphere. In a vacuum, a system is needed to combat this and damp the oscillation. Eddy current damping is used as it minimizes the complexity and improves the ease of analysis due to its passive nature. The improved transient response and control of overshoot offered by active damping come with significant complexity penalty [21] and is not as important

for the steady state thrusters that will use this system. The magnets for the eddy current damper are mounted to two parallel plates on the upper frame. A 1 mm sheet of aluminum attached to the pendulum forms the eddy currents needed to damp the system. The damper is adjustable against a predetermined power dissipation curve by adding or subtracting magnets, allowing it to be both tuneable to a ratio and setup for new thrusters with minimal turnaround time. The estimation for the power dissipated per unit mass, P , depends on the peak magnetic field, B_p , the thickness of the damped aluminium sheet, d , the frequency, f , the resistivity of the material, R , and the density of the material, ρ [22]:

$$P = \frac{\pi^2 B_p^2 d^2 f^2}{6 R \rho} \quad (3)$$

During setup, the system is set to a damping coefficient of >0.4 [2]. This returns the system to steady state quickly and minimizes dynamic amplification of the pendulum response near the stands natural frequency.

F. Calibration

The system for calibration is critical for the overall accuracy of the thrust stand. The sensitivity derived from the calibration data is a first order effect on the accuracy of the final measurement. It should mimic the actual thrust application and measurement as closely as possible to reduce additional systematic errors. The calibration system used here is the most common setup for inverted pendulum thrust stands [2, 15, 20]. Force is applied with the addition of weights attached to a flexible fiber. The fiber attaches to the top of the pendulum in the direction of the thrust vector and drops over a PTFE guide to hang down the rear of the thrust stand in a section covered by the watercooling shroud. The other end is connected to a pulley on a NEMA 8 stepper motor which raises and lowers the weights so they pull the fiber and deflect the pendulum. Several sets of weights on both fine fishing line and cotton thread are used to calibrate depending on the intended thrust level and flexures used. A total of 4 weights are added sequentially to check the linearity of the stand. Future updates to this system to change the weight adding procedure and fiber choice will be discussed in section IIIA.

During experiments, calibration is taken both before and after testing to check for drift and sensitivity changes from heating of both the thrust stand and of the propellant, data and power connections. This is a key point in maintaining the repeatability of the measurement. The calibration procedure for the thrust stand can be seen in fig 6.

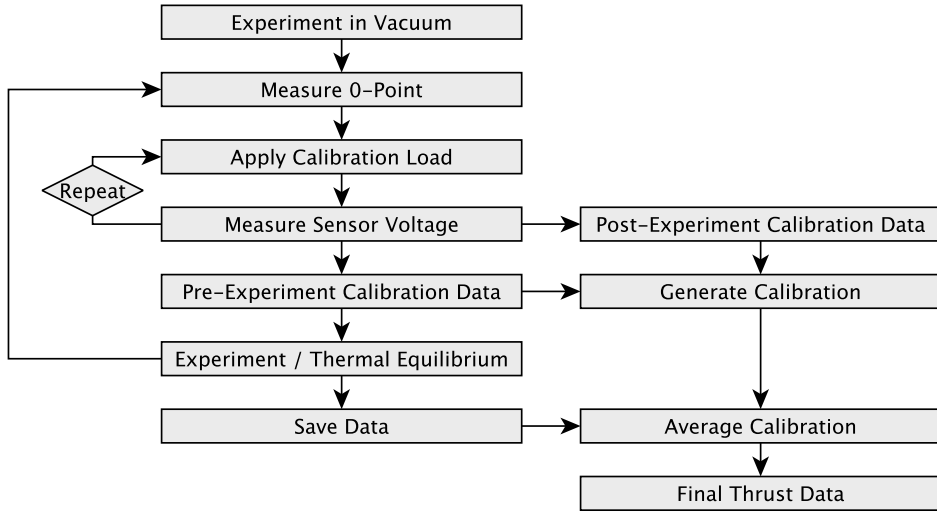


Figure 6: Flow chart showing the standard calibration procedure.

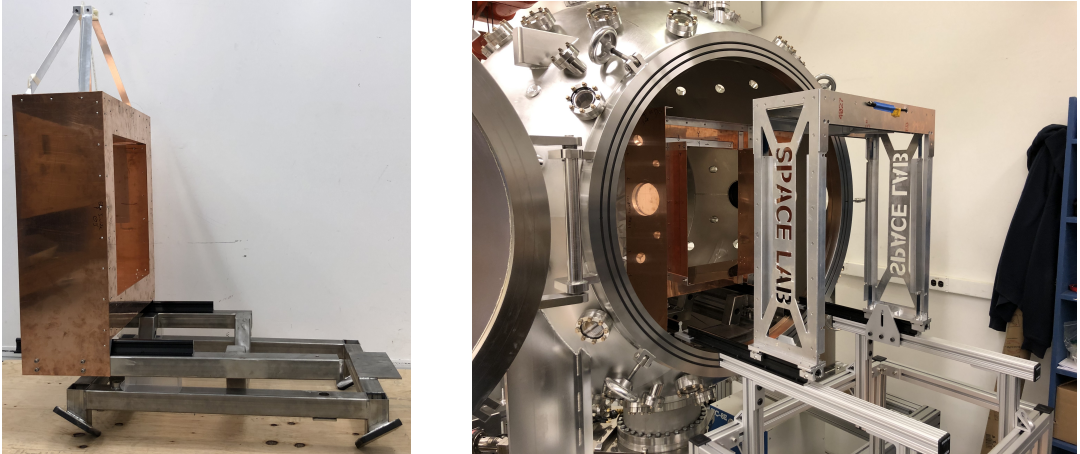


Figure 7: a) The full setup of the thrust stand inside the thermal shroud (water cooling loop not shown). b) The cart with the thrust stand loaded.

G. Watercooling

Electric propulsion systems produce significant heat during operation. The thrust stand is therefore surrounded by a thermal shroud with an integrated watercooling loop, see figure 7a. The shroud is constructed from 1 mm thick 101 copper sheet with 1/4" copper pipe soldered onto the surface. The shroud also protects the interior instruments and calibration systems from the thruster plume and potential sputtering. The thin flexures are particularly sensitive to temperature and must be thermally controlled. Taking into consideration the thermal expansion and change in Young's modulus, the total error in the equivalent spring constant is $3.1 \times 10^{-4} \text{ K}^{-1}$. The flexures should therefore be kept within $\pm 16 \text{ K}$ for an error of 0.5%. To monitor the temperature changes, thermocouples will be used during operation. As the flexures cannot be measured directly, thermocouples will be mounted to the structure that holds the pendulum in place as it has significant thermal contact with the lower flexures, and on the pendulum truss where it contracts the upper flexures.

H. Accessibility and Preparation

In order for the thruster to be set up easily, the stand uses a set of rails that mount the frame to the base within the watercooling shroud. A second set of rails is mounted to a cart outside the chamber allowing the chamber to be opened and the thruster to be wheeled out. The thruster is secured in place both on the cart and in the chamber using two bolts restricting all movement. The propellant, power and data lines have disconnects at the thruster allowing the waterfall to be disconnected before thruster removal.

III. Experimental Results

To determine the efficacy of the design at providing accurate, predictable, and repeatable thrust measurements, end-to-end bench tests were conducted. The thrust stand should produce a linear response to applied force, particularly in the transitions between the modular flexures that allow such a wide range to be tested. The calibration and analysis of the thrust stand used both the in-situ calibration system, described in section II F, and a cold gas thruster. The thruster is a 1/4" stainless steel tube with a 2 mm nozzle attached to the stand and fed by a flexible tube. A compressed air line feeds gas via one of two pressure gauges. Up to 5 psi, a digital pressure gauge with 0.001 psi resolution was used. For tests between 5 and 15 psi an analog gauge is substituted. This gives a predicted range of thrust, F_T between $10 \mu\text{N}$ and 100 mN , using the mass flow rate \dot{m} , exhaust velocity, v_{ex} , nozzle area, A , and the pressures of the exhaust and atmosphere, P_e and P_a :

$$F_T = \dot{m}v_{ex} + A(P_e - P_a) \quad (4)$$

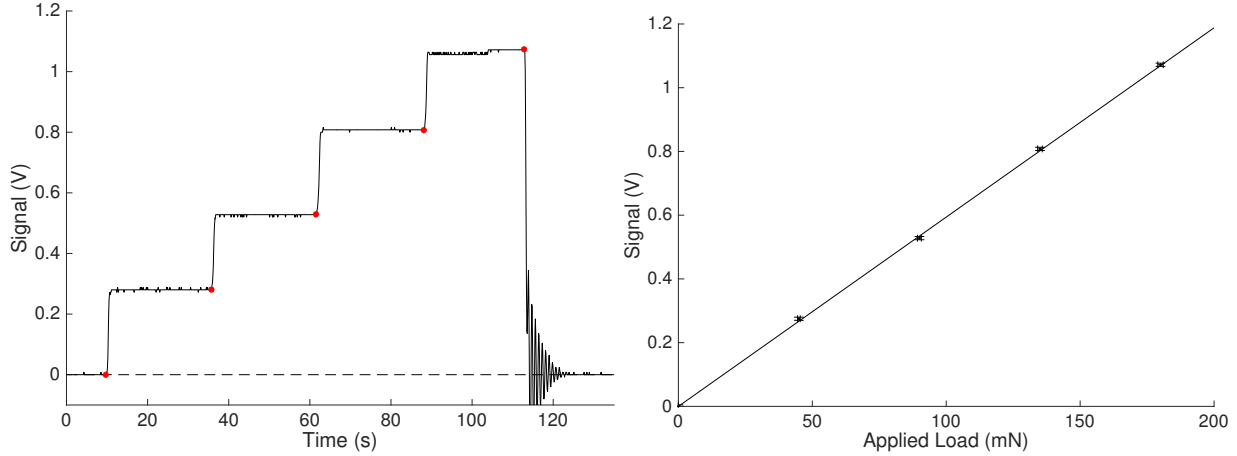


Figure 8: a) The step function generated by the calibration procedure with the data points taken. b) The linear response to the calibration.

The test procedure followed the flow chart in figure 6. For each set of flexures (0.25, 0.38, 0.51, 0.64 mm), a calibration step function and accompanying sensitivity curve was generated. An example of the calibration can be seen in fig 6a. Each mass was loaded and the stand oscillation was allowed to damp over 20 seconds. The value taken for calibration is at the end of each step once it has achieved steady state. Loading the weights on one at a time over several minutes allows the linearity of the response to be checked with each step the same size. The weights were then unloaded and the zero point was checked to confirm that the pendulum had returned to its original position.

The calibration curves for the three stiffest sets of flexures showed good linear response within the uncertainty of the setup, see figure 8. However, some non-linearity and drift of the zero point was seen during testing with the thinnest flexures. Adjustment of the waterfall for the gas line resolved this issue. However an update to the waterfall to allow it to be positioned exactly above the connection of the thruster is ongoing which will ensure that this issue does not continue in future tests.

The signal for each pressure level was averaged over 10 seconds once the pendulum and line pressure were allowed to come to steady state. The pressure was swept over the range several times taking leap-frog measurements to check for zero point drift when the pressure returned to zero. The raw data from each of the runs can be seen in figure 9a. Applying the calibration for each of the sets of data results in figure 9b. The thrust values calculated show a linear increase over the three orders of magnitude measured.

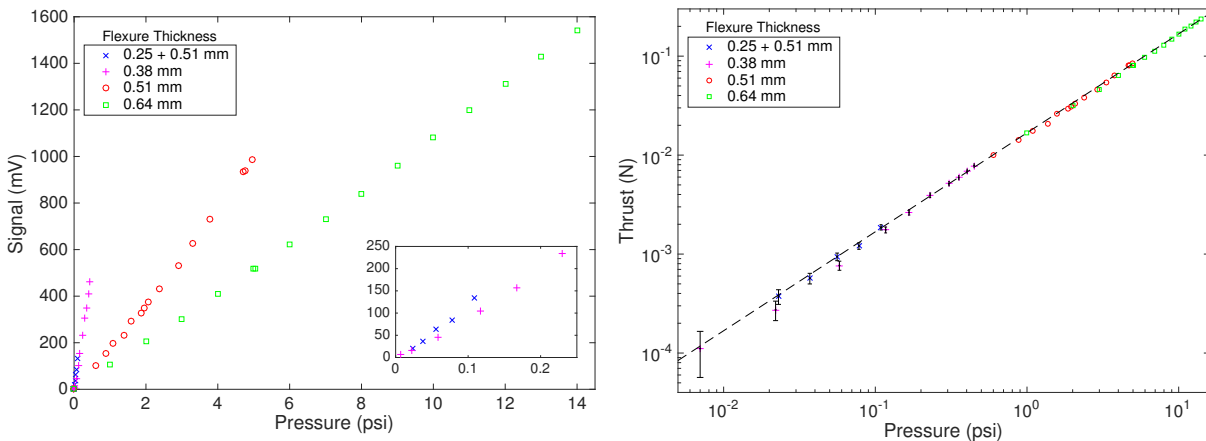


Figure 9: a) Raw signal from the laser for each of the measurements. b) Thrust data calculated from the calibration for each flexure set.

The testing was done outside the chamber due to the mounting of the chamber extension. As the stand was in a well ventilated lab, albeit inside the watercooling shroud, small air currents were enough to create movement in the thrust stand with the most sensitive flexures. As a result the tests were stopped at 100 μN as reliable measurements could no longer be taken due to fluctuations as high as 50 μN .

In the mid range of the stand, between 1 and 30 mN the characteristics of the damped harmonic oscillator were measured with the eddy current damper tuned to an appropriate level. The result is a response curve with a rise time of 0.2 s, peak time of 0.4 s, a maximum overshoot of 24% and a settling time of 1.2 seconds. The damping coefficient, when compared to the analytical model is estimated to be 0.4 - 0.5, within the suggested value by Polk et al. [2]. The response of the pendulum to the applied thrust is very predictable and linear within the small angle approximation used. The analytical model's response matches the experiment data, allowing it can be used to predict the response beyond the tested limits of the experiment and with additional flexure setups.

A. Continued Development

With some continued development, the minor shortcomings seen at the upper and lower ends of the thrust range during this series of experiments can be resolved. The eddy current damper represents an upper limit of effective thrust measurement. When testing the stiffest flexures, at 0.65 mm thick, the overshoot is as high as 81% of the change in deflection with an estimated damping coefficient of < 0.1 , see figure 10a. This presents a risk of the pendulum hitting the stops that limit the pendulum's motion. To increase the available range of the thrust stand at the upper level, a more powerful set of magnets and thicker sheet of aluminum could be used to increase damping as required. Looking beyond the 100 mN tested upper limit, the stiffness of the structure is suitable for thrust levels as high as 1N which could be achieved with the addition of a set of 1 mm flexures.

During calibration testing, some hysteresis was seen in the position of the pendulum when unloading the weights. The middle steps seen in figure 10b should be at the same level, however friction between the PTFE and the fiber causes the motion to stop short. Testing with loading and unloading the test weights, repeating the test and perturbing the stand with the masses loaded shows that the response during the addition of weight is correct and repeatable. However, in the future, the PTFE guide will be changed to a low friction pulley and the flexible fibers potentially replaced with a fine chain to limit the effects of friction and torsion.

At the lower limits of the range tested, air movement in the lab created significant errors with fluctuations in the range of 50 μN and the testing was cut short of finding the true lower limits. Additionally, at lower flexure stiffness, the waterfall affected response more significantly adding non-linear effects. The waterfall used was setup as a prototype for this experiment and did not adequately position the gas line above the thruster. Future iterations of the waterfall head will have a greater range of adjustment to secure the power, data and fluid connections straight above the neutral position.

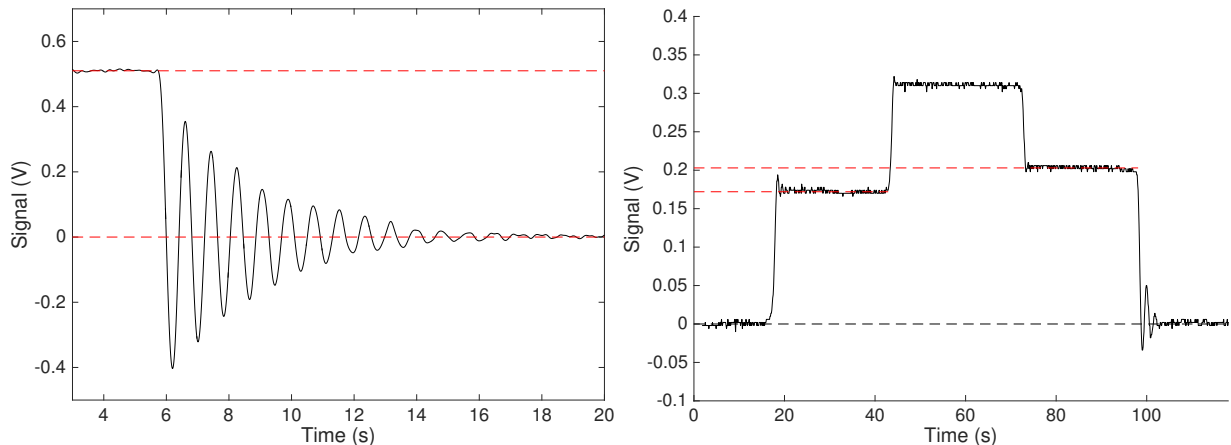


Figure 10: a) Underdamping of the pendulum while testing the response to a step function. b) Hysteresis seen during loading and unloading of the masses during calibration

IV. Conclusion

The analysis and demonstration of SPACE Lab's new compact, modular thrust stand showed success in providing accurate, predictable, and repeatable thrust measurements throughout testing. The stand response showed excellent linearity across the full 100 μN to 100 mN range with good consistency between the flexure setups. With the modifications detailed in section IIIA, repeatable and accurate measurements are likely possible in the sub 100 μN regime. Continued testing in a vacuum environment with the full vibration damping can verify the noise floor which will represent the true limit to low thrust measurement. The range and sensitivity shown by this thrust stand are excellent for the smaller characteristic size. The design falls within the desired region in set out in section II showing reliable thrust measurement can be taken in smaller test facilities.

References

- [1] A Neumann, J Sinske, and HP Harmann. "The 250mN Thrust Balance for the DLR Goettingen EP Test Facility". In: *International Electric Propulsion Conference* (2013), pp. 1–10.
- [2] James E. Polk et al. "Recommended Practice for Thrust Measurement in Electric Propulsion Testing". In: *Journal of Propulsion and Power* 33.3 (2017), pp. 539–555. ISSN: 0748-4658. DOI: 10.2514/1.B35564. URL: <https://arc.aiaa.org/doi/10.2514/1.B35564>.
- [3] Ugur Kokal and Murat Celik. "Development of a mili-Newton level thrust stand for thrust measurements of electric propulsion systems". In: *Proceedings of 8th International Conference on Recent Advances in Space Technologies, RAST 2017* (2017), pp. 31–37. ISSN: 1099-4300. DOI: 10.1109/RAST.2017.8002970.
- [4] T Randolph et al. "Facility effects on stationary plasma thruster testing". In: *International Electric Propulsion Conference* (1993).
- [5] Fernando Mier Hicks. "Characterization on a magnetically levitated testbed for electrospray propulsion systems". In: *MIT Masters Thesis* (2014), pp. 1–82.
- [6] T. W. Haag. "Thrust stand for high-power electric propulsion devices". In: *Review of Scientific Instruments* 62.5 (1991), pp. 1186–1191. ISSN: 00346748. DOI: 10.1063/1.1141998.
- [7] Trevor Moeller and Kurt A. Polzin. "Thrust stand for vertically oriented electric propulsion performance evaluation". In: *Review of Scientific Instruments* 81.11 (2010). ISSN: 00346748. DOI: 10.1063/1.3502463.
- [8] Dan Lev et al. "The technological and commercial expansion of electric propulsion". In: *Acta Astronautica* 159.August 2018 (2019), pp. 213–227. ISSN: 00945765. DOI: 10.1016/j.actaastro.2019.03.058.
- [9] M. R. Drinkwater et al. "GOCE: ESA's first earth explorer core mission". In: *Space Science Reviews* 108.1-2 (2003), pp. 419–432. DOI: 10.16309/j.cnki.issn.1007-1776.2003.03.004.
- [10] Debopam Bhattacherjee et al. "Gearing up for the 21 st century space race". In: *HotNets 2018 - Proceedings of the 2018 ACM Workshop on Hot Topics in Networks* (2018), pp. 113–119. DOI: 10.1145/3286062.3286079.
- [11] M. Martinez-Sanchez and J. E. Pollard. "Spacecraft electric propulsion - An overview". In: *Journal of Propulsion and Power* 14.5 (1998), pp. 688–699. ISSN: 07484658. DOI: 10.2514/2.5331.
- [12] L. Boccaletto and L. D'Agostino. "Design and testing of a micro-newton thrust stand for FEEP". In: *35th Intersociety Energy Conversion Engineering Conference and Exhibit July* (2000).
- [13] Aj Jamison and Ad Ketsdever. "Accurate Measurement of Nano-Newton Thrust for Micropropulsion System Characterization". In: *27th International Electric Propulsion Conference* (2001), pp. 1–14. URL: http://erps.spacegrant.org/uploads/images/images/iepc%7B%5C_%7Darticledownload%7B%5C_%7D1988-2007/2001index/236%7B%5C_%7D1.pdf.
- [14] Manuel Gamero-Castano. "A torsional balance for the characterization of microNewton thrusters". In: *Review of Scientific Instruments* 74.10 (2003), pp. 4509–4514. ISSN: 00346748. DOI: 10.1063/1.1611614.

- [15] Brett Tartler. “Construction and Performance of an Inverted Pendulum Thrust Balance”. In: May 2010 (2010). ISSN: 01663542. DOI: 10.1016/j.antiviral.2010.09.005.
- [16] Leonard Cassady, Andrea Kodys, and Edgar Choueiri. “A Thrust Stand for High-power Steady-state Plasma Thrusters”. In: *38th AIAA/ASME/SAE/ASEE Joint Propulsion Conference Exhibit* (2002). DOI: 10.2514/6.2002-4118. URL: <http://arc.aiaa.org/doi/abs/10.2514/6.2002-4118>.
- [17] N. Nagao et al. “Development of a two-dimensional dual pendulum thrust stand for Hall thrusters”. In: *Review of Scientific Instruments* 78.11 (2007), pp. 8–11. ISSN: 00346748. DOI: 10.1063/1.2815336.
- [18] John K Ziemer. “Performance Measurements Using a Sub-Micronewton Resolution Thrust Stand”. In: *International Electric Propulsion Conference* (2001).
- [19] Jesus Flores et al. “Development of a Torsional Thrust Balance for the Performance of 5-N Class Thrusters”. In: *47th Joint Propulsion Conference & ExhibitJoint Propulsion Conference & Exhibit* August (2011), pp. 1–12. DOI: 10.2514/6.2011-6016.
- [20] Kunming G. Xu and Mitchell L R Walker. “High-power, null-type, inverted pendulum thrust stand”. In: *Review of Scientific Instruments* 80.5 (2009), pp. 1–6. ISSN: 00346748. DOI: 10.1063/1.3125626.
- [21] A D Kodys et al. “An Inverted-Pendulum Thrust Stand for High-Power Electric Thrusters”. In: *Plasma Science and Technology* July (2006).
- [22] F Fiorillo. *Measurement and characterization of magnetic materials*. Elsevier Academic Press, 2004. ISBN: 0-12-257251-3.